VIP Stokes Shift-Engineered Quantum Dots Very Important Paper

Deutsche Ausgabe: DOI: 10.1002/ange.201601198
Internationale Ausgabe: DOI: 10.1002/anie.201601198

Crafting Core/Graded Shell–Shell Quantum Dots with Suppressed Re-absorption and Tunable Stokes Shift as High Optical Gain Materials

*Jaehan Jung, Chun Hao Lin, Young Jun Yoon, Sidney T. Malak, Yaxin Zhai, Edwin L. Thomas, Valy Vardeny, Vladimir V. Tsukruk, and Zhiqun Lin**

Abstract: *The key to utilizing quantum dots (QDs) as lasing media is to effectively reduce non-radiative processes, such as Auger recombination and surface trapping. A robust strategy to craft a set of CdSe/$Cd_{1-x}Zn_xSe_{1-y}S_y$/ZnS core/graded shell–shell QDs with suppressed re-absorption, reduced Auger recombination rate, and tunable Stokes shift is presented. In sharp contrast to conventional CdSe/ZnS QDs, which have a large energy level mismatch between CdSe and ZnS and thus show strong re-absorption and a constrained Stokes shift, the as-synthesized CdSe/$Cd_{1-x}Zn_xSe_{1-y}S_y$/ZnS QDs exhibited the suppressed re-absorption of CdSe core and tunable Stokes shift as a direct consequence of the delocalization of the electron wavefunction over the entire QD. Such Stokes shift-engineered QDs with suppressed re-absorption may represent an important class of building blocks for use in lasers, light emitting diodes, solar concentrators, and parity-time symmetry materials and devices.*

Semiconductor quantum dots (QDs) possess size-dependent optical and electronic properties due to quantum confinement. This opens up opportunities for revolutionary advances in solar cells,[1] lasers,[2] solar concentrators,[3] light-emitting diodes,[4] optical amplifiers,[5] and bioimaging.[6] The solution processability of QDs enabled by capping them with organic ligands renders the easy incorporation of colloidal QDs in polymer matrices and expands the possibilities for the development of scalable and low-cost manufacturing techniques. Among various types of QDs, CdSe QD is one of the most appealing and widely studied inorganic semiconductors due to its optimum band gap corresponding to emission in the visible region. Moreover, their emission wavelength can be readily tuned by varying the size of CdSe QD.[7,8] However, the utilization of CdSe QD in optoelectronic devices is hindered due to unstable optical properties resulting from the surface dangling bonds that act as nonradiative recombination sites. To this end, surface passivation by organic ligands is employed to reduce surface dangling bonds in CdSe QD, thereby leading to enhanced luminescence efficiency and improved photo and colloidal stability.[9] However, the difficulty in passivating the entire surface (that is, anionic and cationic sites) with organic or polymeric ligands still causes chemical degradation or photo-oxidation of QDs.[10] In this context, inorganic surface passivation has been proven to be effective in completely covering the surface of QD, yielding a core–shell architecture. For CdSe QD, the surfaces are often passivated with either ZnS or CdS to establish Type I energy alignment system, where the band gap of CdSe lies within the band gap of the shell material.

It is worth noting that to realize the utility of CdSe QDs as robust lasing media, it is of key importance to reduce ultrafast non-radiative relaxation pathways such as Auger recombination, in which the electron–hole recombination energy is transferred to a third particle such as an electron or a hole that is re-excited to a higher-energy state.[5] The Auger recombination rate depends heavily on the size of CdSe nanocrystals.[11] It has been demonstrated that the implementation of larger CdSe QDs and CdSe QDs with graded shell architecture can reduce the Auger recombination rate.[12] In this context, giant CdSe/CdS core–shell QDs (denoted CdSe/CdS g-QDs in which small CdSe core was passivated by large CdS shell) synthesized by the successive ion layer adsorption and reaction of monolayers (SILAR) method exhibited reduced surface trapping and Auger recombination.[7a,12] Moreover, they displayed the pronounced red-shift of emission peak, which is indicative of the extension of CdSe core wavefunction into the CdS shell region, that is, an increase of the effective size of core.[12] Interestingly, the first absorption peak of CdSe/CdS g-QDs is relatively suppressed as well, due to the absorption primarily from the thick CdS shell as the band gap of CdS is larger than that of CdSe. However, achieving the re-absorption-suppressed CdSe/CdS g-QDs with emission position over the entire visible region is limited due to the large band gap of CdS (for example, 2.42 eV; corresponding to an onset of absorption at 512 nm) compared to CdSe. Furthermore, g-QDs are typically prepared by the SILAR method, which requires time-consuming multiple steps to epitaxially deposit the desired shell material. Clearly, it is highly desirable to develop alternative, simple, yet robust and facile synthetic routes to g-QDs with enhanced photostability and quantum yield.

Herein, we report a viable strategy to craft highly luminescent CdSe/$Cd_{1-x}Zn_xSe_{1-y}S_y$/ZnS core/graded shell–shell QDs with suppressed re-absorption, reduced Auger recombination, and tunable Stokes shift, which are suitable as active and extremely stable gain materials. The plain CdSe

[*] Dr. J. Jung, C. H. Lin, Y. J. Yoon, S. T. Malak, Prof. V. V. Tsukruk, Prof. Z. Lin
School of Materials Science and Engineering
Georgia Institute of Technology, Atlanta, GA 30332 (USA)
E-mail: zhiqun.lin@mse.gatech.edu
Y. Zhai, Prof. V. Vardeny
Department of Physics and Astronomy, University of Utah
Salt Lake City, UT 84112 (USA)
Prof. E. L. Thomas
Department of Materials Science and Nanoengineering
Rice University, Houston, TX 77251 (USA)

Supporting information for this article can be found under: http://dx.doi.org/10.1002/anie.201601198.

QDs with desired emission were first synthesized and used as seeds. The CdSe QD surface was then coated with a $Cd_{1-x}Zn_xSe_{1-y}S_y$ shell possessing a radial chemical composition gradient, forming CdSe/$Cd_{1-x}Zn_xSe_{1-y}S_y$ QDs. Notably, the graded $Cd_{1-x}Zn_xSe_{1-y}S_y$ shell was simply achieved using a one-pot synthesis approach by capitalizing on the difference of chemical reactivity between cadmium oleate and zinc oleate precursors.[13] Subsequently, a ZnS shell was deposited to further passivate the surface of CdSe/$Cd_{1-x}Zn_xSe_{1-y}S_y$ QD via secondary injection of S precursors, yielding robust CdSe/$Cd_{1-x}Zn_xSe_{1-y}S_y$/ZnS core/graded shell–shell QDs. The size and shape of QDs were examined using high-resolution TEM (HRTEM). The absorption and photoluminescence studies of CdSe/$Cd_{1-x}Zn_xSe_{1-y}S_y$/ZnS QDs revealed a dependence of emission peak position on the ZnS shell thickness. These chemical composition gradient QDs possess outstanding photostability as a result of the alleviated lattice strain between CdSe and ZnS due to the judicious incorporation of the $Cd_{1-x}Zn_xSe_{1-y}S_y$ graded shell. Moreover, the Stokes shift (that is, the difference between absorption and emission maxima) of these QDs with the graded shell architecture can be readily engineered by simply further tailoring the thickness of the outermost ZnS shell (that is, red-shift with an increase of ZnS shell thickness), which cannot be observed in conventional CdSe/ZnS QDs owing to their large energy level mismatch.[14] It is also notable that CdSe/$Cd_{1-x}Zn_xSe_{1-y}S_y$/ZnS QDs are advantageous over giant CdSe/CdS QDs as ZnS has a larger band gap than CdS and therefore offers a high degree of tunability in selecting the emission position in the visible region due to the suppression of re-absorption. In comparison to plain CdSe QDs, all CdSe/$Cd_{1-x}Zn_xSe_{1-y}S_y$/ZnS QDs with different emission positions exhibited an extended lifetime, signifying a reduced Auger recombination rate as a direct consequence of the delocalization of the electron wave function over the entire QD.

Highly luminescent CdSe/$Cd_{1-x}Zn_xSe_{1-y}S_y$ core–shell QDs were synthesized by passivating the surface of a plain CdSe QD core with the graded $Cd_{1-x}Zn_xSe_{1-y}S_y$ shell. The radially graded $Cd_{1-x}Zn_xSe_{1-y}S_y$ shell on the CdSe QD surface was formed via a careful control of the ratio of Cd and Zn precursors. A further epitaxial growth of the ZnS shell through secondary injection of S precursors (S/TOP) yielded CdSe/$Cd_{1-x}Zn_xSe_{1-y}S_y$/ZnS core/graded shell–shell QDs (see the Supporting Information, Experimental Section). It is worth noting that the graded $Cd_{1-x}Zn_xSe_{1-y}S_y$ shell was achieved by simply exploiting the difference in chemical reactivity between cadmium and zinc precursors (that is, Cd-oleate and Zn-oleate; see the Supporting Information, Experimental Section). Specifically, the weaker binding energy of oleic acid with Cd^{2+} than that with Zn^{2+} resulted in a higher reactivity of Cd-oleate than Zn-oleate during the crystal growth reaction.[13,15] Consequently, the formation of CdSe and CdS is more favorable than ZnSe and ZnS, yielding $Cd_{1-x}Zn_xSe_{1-y}S_y$ shell with a gradual increase of Zn and S ratio over Cd and Se.[13] It is important to note that the energy level of the resulting CdSe/$Cd_{1-x}Zn_xSe_{1-y}S_y$/ZnS QDs with the radial gradient chemical composition can be regarded as a graded smooth energy band alignment rather than the sharp interface as in conventional CdSe/ZnS QDs, as depicted in the Supporting Information, Scheme S1. Moreover, the graded shell architecture can effectively reduce the interfacial lattice strain between CdSe and ZnS (that is, a large, 12% lattice mismatch between CdSe and ZnS), which would otherwise lead to a dramatic increase in trapping sites with the increase of ZnS shell thickness.[7a,16]

Figure 1 shows HRTEM images of the chemical composition gradient QDs prepared at 250°C using 2.3 ± 0.1 nm green-emitting CdSe QDs as seeds. The diameter of QDs increased from 2.3 ± 0.1 nm for the as-prepared CdSe QD

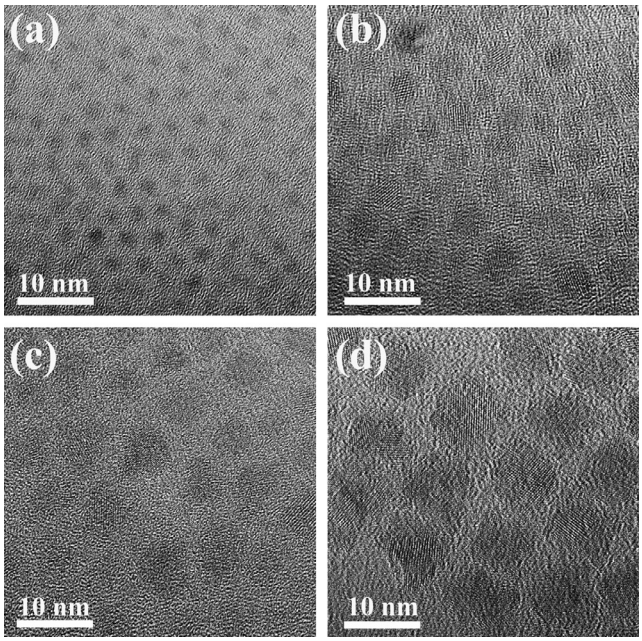

Figure 1. TEM images of a) plain CdSe QDs as core (green-emitting; $D = 2.3$ nm), b) CdSe/$Cd_{1-x}Zn_xSe_{1-y}S_y$ QDs ($D = 4.4$ nm), c) CdSe/$Cd_{1-x}Zn_xSe_{1-y}S_y$/ZnS QDs ($D = 6.0$ nm), and d) CdSe/$Cd_{1-x}Zn_xSe_{1-y}S_y$/ZnS QDs ($D = 8.4$ nm). All chemical composition gradient QDs were synthesized using 2.3-nm green-emitting CdSe QDs as seeds at 250°C.

core (Figure 1a) to 4.4 ± 0.2 nm for the CdSe/$Cd_{1-x}Zn_xSe_{1-y}S_y$ QDs (Figure 1b) to 6.0 ± 0.2 nm for the CdSe/$Cd_{1-x}Zn_xSe_{1-y}S_y$/ZnS QDs (grown for 30 min), and eventually to 8.4 ± 0.4 nm for CdSe/$Cd_{1-x}Zn_xSe_{1-y}S_y$/ZnS QDs (grown for 90 min; see the Supporting Information, Experimental Section), clearly suggesting the controlled deposition of $Cd_{1-x}Zn_xSe_{1-y}S_y$ graded shell and subsequent ZnS shell. The CdSe/$Cd_{1-x}Zn_xSe_{1-y}S_y$/ZnS QDs also possessed good crystallinity as revealed by TEM (for example, Figure 1d).

The optical properties of as-synthesized CdSe/$Cd_{1-x}Zn_xSe_{1-y}S_y$/ZnS QDs were investigated by absorption and photoluminescence spectroscopy measurements. The conventional CdSe/ZnS QDs were also synthesized and used as control for comparative studies. To scrutinize the effect of the graded shell on the change in absorption (namely, the first absorption peak) and emission properties (emission peak) and quantum yield (QY), plain CdSe QDs were passivated with both a graded shell ($Cd_{1-x}Zn_xSe_{1-y}S_y$) and a graded shell–shell ($Cd_{1-x}Zn_xSe_{1-y}S_y$/ZnS), respectively. The

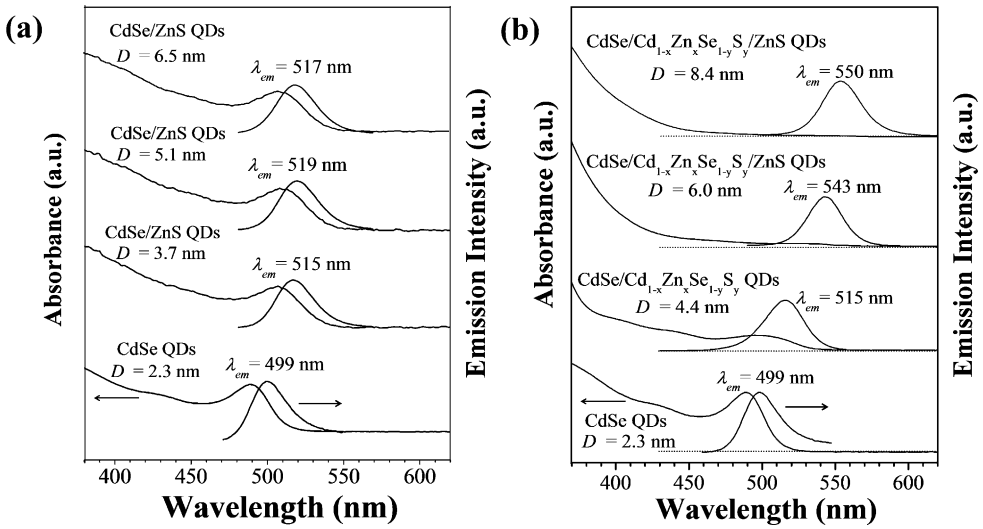

Figure 2. The absorption and emission spectra of a) CdSe/ZnS QDs and b) CdSe/$Cd_{1-x}Zn_xSe_{1-y}S_y$/ZnS QDs, in which the diameter of originally green-emitting CdSe QD core, *D* is 2.3 nm. All CdSe/ZnS, CdSe/$Cd_{1-x}Zn_xSe_{1-y}S_y$, and CdSe/$Cd_{1-x}Zn_xSe_{1-y}S_y$/ZnS QDs were grown from green-emitting CdSe QD at 250 °C.

absorption and emission spectra of tetradecylphosphonic acid (TDPA)-capped CdSe QDs ($D = 2.3$ nm; green-emitting; Supporting Information, Experimental Section) with the first absorption peak at 488 nm, emission peak, λ_{em} at 500 nm, emission full width at half maximum (FWHM) at 29 nm, and QY of 2.2% are shown in Figure 2a and 2b. We note that TDPA was utilized for the synthesis of CdSe core QDs as it enables the preparation of CdSe QDs with a narrow size distribution.[17] After passivation of the CdSe core with $Cd_{1-x}Zn_xSe_{1-y}S_y$ graded shell and ZnS shell, the QYs of both QDs increased, that is, from 2.2% for CdSe QD core to 40.0% for CdSe/$Cd_{1-x}Zn_xSe_{1-y}S_y$ QDs ($D = 4.4$ nm; Figure 2b), and from 2.2% for CdSe QD core to 36.7% for conventional CdSe/ZnS QDs ($D = 3.7$ nm; Figure 2a), respectively, which was due to the reduction in surface dangling bonds.[16,18] The FWHM of the emission peaks was maintained in both QDs (that is, 32 nm; Supporting Information, Table S1) as highly monodisperse TDPA-capped CdSe QDs were employed as seeds. The emission peak position of CdSe/$Cd_{1-x}Zn_xSe_{1-y}S_y$ QDs and CdSe/ZnS QDs shifted from $\lambda_{em} = 499$ nm for CdSe QDs to $\lambda_{em} = 515$ nm in both cases. This can possibly be attributed to the increase in the size of the CdSe core during the reaction due to the existence of residue Cd and Se precursors.[16]

Notably, conventional CdSe/ZnS core–shell QDs without the gradient shell exhibited a constant emission position (that is, λ_{em} is circa 517 nm; Figure 2a) regardless of the increase of ZnS shell thickness. The lack of dependence between the emission position and ZnS shell thickness is due to large energy level difference between CdSe and ZnS (Supporting Information, Scheme S1a), which leads to the strong localization of electrons solely in the CdSe core (Type I behavior; Figure 2a and Supporting Information, Table S1). Specifically, conventional CdSe/ZnS QDs with different shell thickness were prepared as a control group by changing the reaction time from 10 min ($D = 3.7$ nm; Figure 2a) to 30 min ($D = 5.1$ nm; Figure 2a) to 90 min ($D = 6.5$ nm; Figure 2a). Clearly, even CdSe/ZnS QDs with a *D* of 6.5 nm corresponding to 7 monolayers of ZnS shell (a monolayer of ZnS is 3.1 Å between consecutive planes along the [002] axis in bulk wurtzite ZnS)[16] did not exhibit a red-shift of the emission peak. In stark contrast, the emission peak of chemical composition gradient QDs displayed a larger red-shift of emission ($\lambda_{em} = 543$ nm for CdSe/$Cd_{1-x}Zn_xSe_{1-y}S_y$/ZnS with $D = 6.0$ nm) and further up to $\lambda_{em} = 550$ nm for CdSe/$Cd_{1-x}Zn_xSe_{1-y}S_y$/ZnS with $D = 8.4$ nm; Supporting Information, Table S1), and quite intriguingly, their first absorption peaks were greatly suppressed (Figure 2b). As evidenced by the TEM measurements (Figure 1c,d), the increased diameter of QDs suggested the successful passivation by the outermost ZnS shell, and thus possibly renders the delocalization of the electron wave function over the entire CdSe/$Cd_{1-x}Zn_xSe_{1-y}S_y$/ZnS QDs because of the graded energy level alignment (Supporting Information, Scheme S1b),[3,12] thereby leading to the emission red-shift. Therefore, compared to conventional CdSe/ZnS QDs, the enhanced Stokes shift in CdSe/$Cd_{1-x}Zn_xSe_{1-y}S_y$/ZnS QDs can be ascribed to an increase of the effective core size of QDs through careful energy level engineering, enabling the extension of the electron wave function over the entire core/grade shell–shell QDs. However, the electron wavefunction is strongly confined within the CdSe core in the case of conventional CdSe/ZnS QDs. It is also worth noting that the absorption onset of CdSe/$Cd_{1-x}Zn_xSe_{1-y}S_y$/ZnS QDs was found to be around 400 nm, which is indicative of the band gap of ZnS (Figure 2b).[19]

As noted above, the advantage of CdSe/$Cd_{1-x}Zn_xSe_{1-y}S_y$/ZnS QDs over CdSe/CdS g-QDs lies in the fact that such chemical composition gradient QDs with emissions across the entire visible region can be crafted due to the larger band gap of ZnS (that is, 3.54 eV corresponding to the absorption onset at 350 nm) in comparison to that of CdS (2.42 eV corresponding to the absorption onset at 512 nm). However, for CdSe/CdS g-QDs, such full visible-region emission is not possible (for example, blue- and green-emitting QDs cannot be attained) as the emission at wavelength below 512 nm will be re-absorbed by the CdS shell. In contrast, the careful control of thickness and composition of the graded shell and outermost ZnS shell may render the ability to form green-emitting CdSe/$Cd_{1-x}Zn_xSe_{1-y}S_y$/ZnS core/grade shell–shell QDs with suppressed re-absorption by imparting a larger Stokes shift, as the absorption onset for the ZnS shell is below the blue wavelength (that is, 350 nm). Thus, it is not surprising

that CdSe/$Cd_{1-x}Zn_xSe_{1-y}S_y$/ZnS QDs with different emissions position and suppressed re-absorption were successfully synthesized by simply employing a CdSe core of different size (Figure 3). Specifically, plain CdSe QDs of 2.3 nm (green-

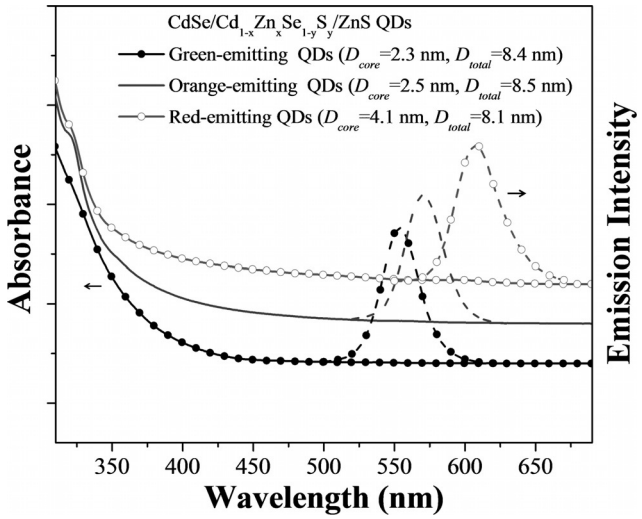

Figure 3. Absorption and photoluminescence spectra of green-, orange-, and red-emitting CdSe/$Cd_{1-x}Zn_xSe_{1-y}S_y$/ZnS QDs synthesized by employing green-emitting CdSe QD ($D = 2.3$ nm), green-emitting CdSe QD ($D = 2.5$ nm), and red-emitting CdSe QD ($D = 4.1$ nm) as seeds.

emitting), 2.5 nm (also green-emitting), and 4.1 nm (red-emitting) in diameter were utilized as seeds to produce green-, orange-, and red-emitting CdSe/$Cd_{1-x}Zn_xSe_{1-y}S_y$/ZnS QDs, respectively (digital images in Figure S1 a–c). The diameters of plain CdSe QD cores were calculated based on their first absorption peak ($\lambda_{1st,abs} = 499$ nm, 520 nm, and 588 nm, respectively)[9] and can be verified by TEM (for example, 2.3 nm CdSe QD as shown in Figure 1 a). The diameters of the resulting green-, orange-, and red-emitting CdSe/$Cd_{1-x}Zn_xSe_{1-y}S_y$/ZnS QDs were 8.4 ± 0.3 nm, 8.5 ± 0.3 nm, and 8.1 ± 0.3 nm, respectively, as measured from TEM analysis (Supporting Information, Figure S1 d–f).

To further examine the emission properties of chemical composition gradient QDs, the kinetics of the transient photobleaching (PB) of the ground state absorption due to the photogenerated excitons in all QDs were measured (Figure 4). All samples were pumped at 400 nm (3.1 eV) with a pulsed excitation duration of about 100 fs, and the PB decay kinetics were probed in the range of their first absorption band, namely, at 547 nm (2.27 eV), 467 nm (2.56 eV), 481 nm (2.58 eV), and 500 nm (2.48 eV) for the CdSe QDs, green-, orange-, and red-emitting CdSe/$Cd_{1-x}Zn_xSe_{1-y}S_y$/ZnS QDs, respectively. All transient decays were fitted with $A\exp(-t/\tau) + C$, and the best fitting parameters of measured QDs are summarized in the Supporting Information, Table S2. Figure 4 shows that the transient PB of plain CdSe QDs decayed with a short lifetime of about 180 ps (Supporting Information, Table S2). Clearly, all chemical composition gradient QDs exhibited longer lifetimes than plain CdSe QDs (Supporting Information, Table S2). In agreement with the

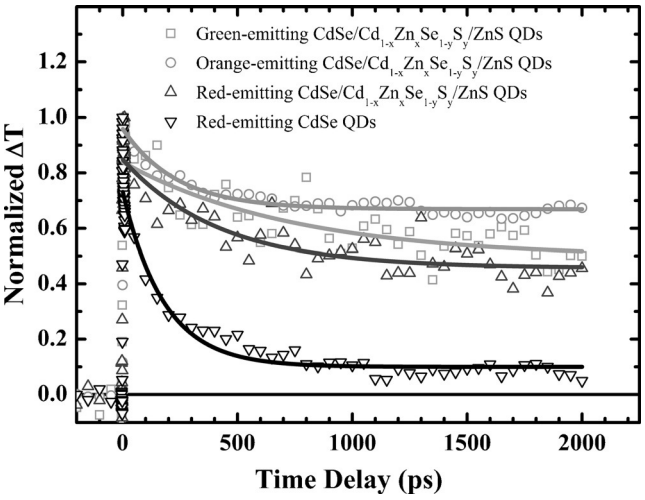

Figure 4. Normalized decay kinetics of photobleaching (PB) of the ground-state absorption up to 2000 ps for red-emitting CdSe core QDs ($D = 4.1$ nm) (▽), red-emitting CdSe/$Cd_{1-x}Zn_xSe_{1-y}S_y$/ZnS QDs ($D = 8.1$ nm) (△), orange-emitting CdSe/$Cd_{1-x}Zn_xSe_{1-y}S_y$/ZnS QDs ($D = 8.5$ nm) (○), and green-emitting CdSe/$Cd_{1-x}Zn_xSe_{1-y}S_y$/ZnS QDs ($D = 8.4$ nm) (□). The solid lines are the fitting to the symbols using an exponential decay superimposed on a constant due to long-lived trapped excitons.

pronounced larger Stokes shift, the longer recombination lifetime strongly supports that the underlying mechanism is due to the delocalization of the electron over the entire CdSe/$Cd_{1-x}Zn_xSe_{1-y}S_y$/ZnS QDs as the Auger recombination rate is proportional to the QD volume.[11,20]

In summary, we developed a robust and facile one-pot synthesis strategy to craft chemical composition gradient CdSe/$Cd_{1-x}Zn_xSe_{1-y}S_y$/ZnS QDs by passivating the surface of CdSe QD core with a $Cd_{1-x}Zn_xSe_{1-y}S_y$ graded shell, followed by an outermost ZnS shell. The resulting CdSe/$Cd_{1-x}Zn_xSe_{1-y}S_y$/ZnS QDs carry intriguing attributes over conventional CdSe/ZnS QDs, including enhanced photoemission resulting from suppressed re-absorption, reduced Auger recombination, and tunable Stokes shift. The first absorption peak of these QDs with the emission in visible region was suppressed due to passivation by the larger band gap of the ZnS shell with an absorption onset of 400 nm. The influence of shell thickness on the variation of Stokes shift and the suppression of the first absorption peak were scrutinized by UV/Vis and PL spectroscopies and compared with conventional CdSe/ZnS QD counterparts. The marked red-shift of emission peak in CdSe/$Cd_{1-x}Zn_xSe_{1-y}S_y$/ZnS QDs with the increase of shell thickness was indicative of the delocalization of the electron wave function over the entire QD due to the incorporation of the graded $Cd_{1-x}Zn_xSe_{1-y}S_y$ shell, leading to a continuous energy level change from CdSe to ZnS. This contrasts sharply to the constant emission peak independent of ZnS thickness seen in conventional CdSe/ZnS QDs. As such, these QDs with graded architecture may offer an effective means of tailoring the Stokes shift of QDs with engineered properties for applications in lasers, LEDs, solar concentrators, and parity-time symmetry materials and devices.

Acknowledgements

Financial support is acknowledged from the Air Force Office of Scientific Research FA9550-14-1-0037 (Synthetic Photonics Multidisciplinary University Research Initiative).

Keywords: Auger recombination · CdSe quantum dots · core/graded shell–shell quantum dots · optoelectronics · Stokes shift

How to cite: *Angew. Chem. Int. Ed.* **2016**, *55*, 5071 – 5075
Angew. Chem. **2016**, *128*, 5155 – 5159

[1] a) J. Jung, X. Pang, C. Feng, Z. Lin, *Langmuir* **2013**, *29*, 8086 – 8092; b) X. Xin, B. Li, J. Jung, Y. J. Yoon, R. Biswas, Z. Lin, *Part. Part. Syst. Charact.* **2015**, *32*, 80 – 90; c) J. Jung, Y. J. Yoon, M. He, Z. Lin, *J. Polym. Sci. Part B* **2014**, *52*, 1641 – 1660; d) M. He, F. Qiu, Z. Lin, *J. Phys. Chem. Lett.* **2013**, *4*, 1788 – 1796; e) J. Xu, J. Wang, M. Mitchell, P. Mukherjee, M. Jeffries-El, J. W. Petrich, Z. Lin, *J. Am. Chem. Soc.* **2007**, *129*, 12828 – 12833.

[2] C. Dang, J. Lee, C. Breen, J. S. Steckel, S. Coe-Sullivan, A. Nurmikko, *Nat. Nanotechnol.* **2012**, *7*, 335 – 339.

[3] F. Meinardi, A. Colombo, K. A. Velizhanin, R. Simonutti, M. Lorenzon, L. Beverina, R. Viswanatha, V. I. Klimov, S. Brovelli, *Nat. Photonics* **2014**, *8*, 392 – 399.

[4] Q. Sun, Y. A. Wang, L. S. Li, D. Wang, T. Zhu, J. Xu, C. Yang, Y. Li, *Nat. Photonics* **2007**, *1*, 717 – 722.

[5] S. A. Ivanov, J. Nanda, A. Piryatinski, M. Achermann, L. P. Balet, I. V. Bezel, P. O. Anikeeva, S. Tretiak, V. I. Klimov, *J. Phys. Chem. B* **2004**, *108*, 10625 – 10630.

[6] Y. Zhang, Y. Li, X.-P. Yan, *Small* **2008**, *5*, 185 – 189.

[7] a) R. Xie, U. Kolb, J. Li, T. Basché, A. Mews, *J. Am. Chem. Soc.* **2005**, *127*, 7480 – 7488; b) J. Xu, J. Xia, J. Wang, J. Shinar, Z. Lin, *Appl. Phys. Lett.* **2006**, *89*, 133110; c) D. Zimnitsky, C. Jiang, J. Xu, Z. Lin, L. Zhang, V. V. Tsukruk, *Langmuir* **2007**, *23*, 10176 – 10183; d) D. Zimnitsky, C. Jiang, J. Xu, Z. Lin, V. V. Tsukruk, *Langmuir* **2007**, *23*, 4509 – 4515.

[8] a) J. Xu, J. Xia, Z. Lin, *Angew. Chem. Int. Ed.* **2007**, *46*, 1860 – 1863; *Angew. Chem.* **2007**, *119*, 1892 – 1895; b) J. Wang, J. Xu, M. D. Goodman, Y. Chen, M. Cai, J. Shinar, Z. Lin, *J. Mater. Chem.* **2008**, *18*, 3270 – 3274; c) X. Pang, L. Zhao, W. Han, X. Xin, Z. Lin, *Nat. Nanotechnol.* **2013**, *8*, 426 – 431; d) B. Li, W. Han, B. Jiang, Z. Lin, *ACS Nano* **2014**, *8*, 2936 – 2942.

[9] W. W. Yu, L. Qu, W. Guo, X. Peng, *Chem. Mater.* **2003**, *15*, 2854 – 2860.

[10] H. Zhang, J. Jang, W. Liu, D. V. Talapin, *ACS Nano* **2014**, *8*, 7359 – 7369.

[11] V. I. Klimov, A. A. Mikhailovsky, S. Xu, A. Malko, J. A. Hollingsworth, C. A. Leatherdale, H. J. Eisler, M. G. Bawendi, *Science* **2000**, *290*, 314 – 317.

[12] Y. Chen, J. Vela, H. Htoon, J. L. Casson, D. J. Werder, D. A. Bussian, V. I. Klimov, J. A. Hollingsworth, *J. Am. Chem. Soc.* **2008**, *130*, 5026 – 5027.

[13] W. K. Bae, K. Char, H. Hur, S. Lee, *Chem. Mater.* **2008**, *20*, 531 – 539.

[14] C. She, I. Fedin, D. S. Dolzhnikov, A. Demortière, R. D. Schaller, M. Pelton, D. V. Talapin, *Nano Lett.* **2014**, *14*, 2772 – 2777.

[15] W. K. Bae, M. K. Nam, K. Char, S. Lee, *Chem. Mater.* **2008**, *20*, 5307 – 5313.

[16] B. O. Dabbousi, J. Rodriguez-Viejo, F. V. Mikulec, J. R. Heine, H. Mattoussi, R. Ober, K. F. Jensen, M. G. Bawendi, *J. Phys. Chem. B* **1997**, *101*, 9463 – 9475.

[17] Z. A. Peng, X. Peng, *J. Am. Chem. Soc.* **2001**, *123*, 183 – 184.

[18] P. Reiss, J. Bleuse, A. Pron, *Nano Lett.* **2002**, *2*, 781 – 784.

[19] D. V. Talapin, A. L. Rogach, A. Kornowski, M. Haase, H. Weller, *Nano Lett.* **2001**, *1*, 207 – 211.

[20] Y.-F. Chen, M. S. Fuhrer, *Phys. Rev. Lett.* **2005**, *95*, 236803.

Received: February 3, 2016
Published online: March 15, 2016

